Rice caryopsis development: Dynamic changes in different cell layers

Xiaoba Wu, Jinxin Liu, Dongqi Li and Chun-Ming Liu*

Key Laboratory of Plant Molecular Physiology, Institute of Botany, Chinese Academy of Sciences, Beijing 100093, China.
*Correspondence: cmliu@ibcas.ac.cn

Abstract   Rice caryopsis as one of the most important food sources for humans has a complex structure that is composed of maternal tissues including the pericarp and testa and filial tissues including the endosperm and embryo. Although rice caryopsis studies have been conducted previously, a systematic characterization throughout the entire developmental process is still lacking. In this study, detailed morphological examinations of caryopses were made during the entire 30-day developmental process. We observed some rapid changes in cell differentiation events and cataloged how cellular degeneration processes occurred in maternal tissues. The differentiations of tube cells and cross cells were achieved by 9 days after pollination (DAP). In the testa, the outer integument was degenerated by 3 DAP, while the outer layer of the inner integument degenerated by 7 DAP. In the nucellus, all tissues with the exception of the nucellar projection and the nucellar epidermis degenerated in the first 5 DAP. By 21 DAP, all maternal tissues, including vascular bundles, the nucellar projection and the nucellar epidermal cells were degenerated.

In summary, this study provides a complete atlas of the dynamic changes in cell differentiation and degeneration for individual maternal cell layers of rice caryopsis.

INTRODUCTION

Rice is one of the most important staple food crops in the world (http://faostat.fao.org) and is consumed by humans as either unpolished brown rice or as polished white rice. As the first monocotyledonous species with a sequenced genome, rice has also been the pre-eminent cereal model for functional genomics and studies of domestication and genome evolution (Goff et al. 2002; Yu et al. 2002; Sang and Ge 2013). The rice grain has a complex structure derived from a floret with a caryopsis that is encased by the lemma and palea (Zee 1972; Gu et al. 2002; Yoshida and Nagato 2011). The caryopsis consists of three genetically distinct components: (i) the diploid maternal tissues including the pericarp, testa and nucellus; (ii) the triploid filial endosperm tissue; and (iii) the diploid filial embryo tissue. All these tissues in a mature caryopsis, with the exception of the embryo and the aleurone, are dead (Krishnan and Dayanandan 2003; Saulnier et al. 2012). Although caryopsis development in different cereal species share some common characteristics, distinct features have been reported in transfer cells (Zee 1972), the aleurone layer (Bosnes et al. 1992) and the storage production accumulations (Opanowicz et al. 2011).

Several morphological studies have been conducted with rice embryos (Jones and Rost 1989) and endosperms (Becraft 2011; Wang et al. 2012). To a lesser extent, there have also been studies of the pericarp and the testa (Zee 1972; Gu et al. 2002; Krishnan and Dayanandan 2003). The pericarp in rice has three vascular bundles, a major one located at the dorsal side and two minor ones at the lateral sides (Krishnan and Dayanandan 2003). The dorsal vascular bundle plays a major role in delivering water, minerals and photosynthesis assimilates to the developing caryopsis (Oparka and Gates 1981; Krishnan and Dayanandan 2003). The cell wall invertase *CIN2/GIF1* expressed in the dorsal vascular bundle may function to hydrolyze sucrose delivered by the phloem to fructose and glucose, since mutation of this gene led to defected grain filling (Wang et al. 2008a; Wang et al. 2008b). The integument in the ovary consists of a two-layer outer integument and a two-layer inner integument (Krishnan and Dayanandan 2003). The outer integument degenerates within 2 days after pollination (DAP), while the degeneration of inner integument is variable depending on the rice cultivars (Krishnan and Dayanandan 2003). It is known that the degeneration of the nucellar projection, which is located adjacent to the dorsal vascular bundle, is critically important for grain filling (Yin and Xue, 2012; Yang et al. 2012). Cells in nucellar epidermis, characterized by ribs of wall-thickening, may function to transport assimilates to the endosperm and embryo (Ellis and Chaffey 1987; Krishnan and Dayanandan 2003). We have showed recently that *NF-YB1* transcription factor gene expressed in the dorsal aleurone of rice plays a critical role in regulating the expressions of three sucrose transports, allowing sucrose to be loaded directly to

the developing starchy endosperm (Bai et al. 2015). In mature rice caryopsis, the testa derived from integuments and nucellar tissues is fused tightly to the pericarp (Evers and Millar 2002; Krishnan and Dayanandan 2003). It has been proposed that coordinated physiological interactions among different tissues of rice caryopses are crucial for grain filling (Lopes and Larkins 1993), although the fine details of the morphological and molecular mechanism underlying this complicated process remain largely unknown.

This study examined cytohistological changes in the rice caryopsis from anthesis through to the final formation of a mature grain, and particular attention was paid to differentiation and degeneration processes that occurred in maternal tissues. We show that, during the 30-day developmental process, individual maternal tissues in the rice caryopsis exhibit dynamic changes in cell size, morphology, starch grain accumulation, and cell wall thickening. More strikingly, we observed highly regulated cell degeneration processes in these tissues at discrete time points.

RESULTS

The rice grain
Morphological and cytohistological analyses were carried out for the caryopses of rice (*Oryza sativa* L. ssp. *japonica*, cultivar Zhonghua 11) grown in a net-protected experimental field in Beijing, China, from May 20 to October 10. The temperature during this period ranged from 22 °C to 35 °C during the day and from 18 °C to 28 °C during the night. The anthesis date of each floret was marked on the surface of the lemma using a marker, and samples were collected and examined on a daily basis throughout the 30-day period of caryopsis development. Under these conditions, it took 30 ± 3 days from anthesis to the formation of a mature grain (Figure 1A, B). We observed that major extension of the rice caryopsis along the long axis occurred from 0 to 6 DAP, while major expansion along the transversal axis occurred between 3 and 8 DAP (Figure 1A, B).

We first examined the structure of the mature rice grain. The term 'grain', as illustrated in Figure 1C and D, refers to a complex structure consisting of two bracts called the lemma (the outer one) and the palea (the inner one), and a caryopsis (a fruit). In the mature grain, the palea and the lemma are tightly interlaced with each other through specialized trichomes formed at their edges to enclose the caryopsis. The palea and lemma are physically separable from the caryopsis (Figure 1C), while the pericarp (the fruit tissue), the testa (the seed coat), the embryo, and the endosperm are tightly fused together (Figure 1C).

As shown in Figure 1C, modern rice processing involves two sequential steps: dehusking and polishing. During dehusking, the palea and the lemma are removed to
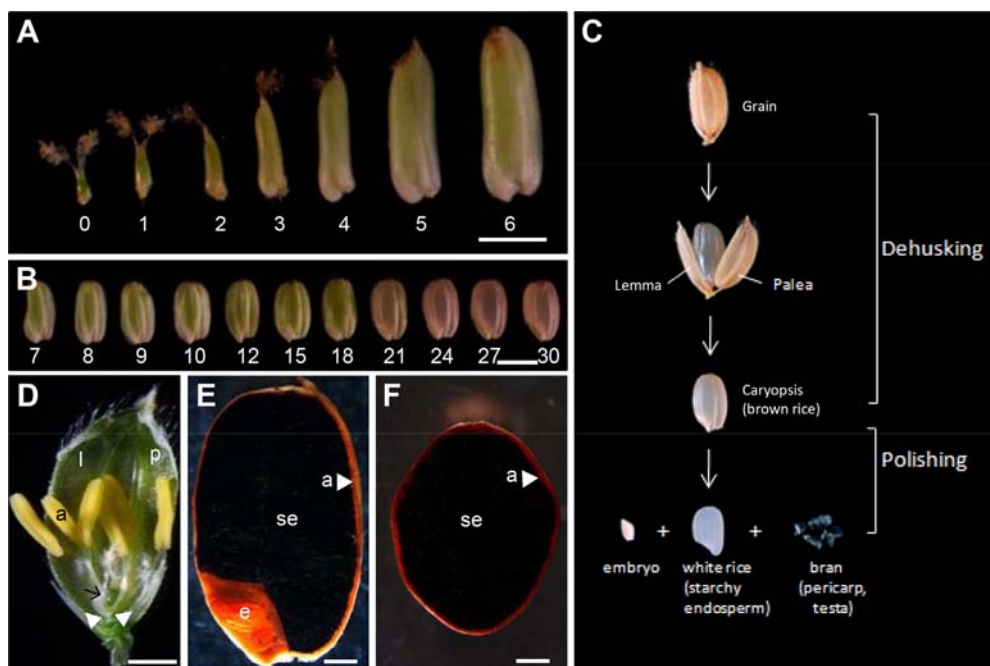
Figure 1. General structure of the rice caryopsis
(A, B) Rice caryopsis development from 0 to 6 days after pollination (DAP) **(A)** and from 7 to 30 DAP **(B)**. Numbers below denote the DAP. Note the rapid elongation of the caryopsis in the first 6 DAP; the major period of expansion occurred between 3 and 8 DAP. **(C)** Two-step milling of the rice grain: dehusking and polishing. Dehusking removes the lemma and palea to produce brown rice; polishing removes the pericarp, testa, and the embryo. **(D)** A mature rice floret. Arrowheads indicate lodicules, the arrow indicates the ovary. a, anther; l, lemma; p, palea. **(E, F)** Longitudinally **(E)** and transversely sectioned **(F)** mature rice caryopsis, stained with Sudan Red IV (orange-red) for lipids and Lugo (black) for starch. Note that lipids are accumulated mainly in the aleurone and the embryo, while starch is accumulated mainly in the starchy endosperm. Arrowheads indicates the aleurone layer. a, aleurone; se, starchy endosperm; e, embryo. Scale bars = 1 mm **(A, B, D)**; 0.5 mm **(E, F)**.

releasethe caryopsis. During polishing, all of the maternal tissues, including the pericarp and the testa, and filial tissues including the aleurone and the embryo are removed as bran, finally producing white rice, which consists mostly of the starchy endosperm (Figure 1C). In many countries, the entire caryopsis is consumed by humans as brown rice without further polishing. Starch is the major component in the starchy endosperm (stained in brown/black by Lugo; Figure 1E, F). Storage proteins are accumulated in both aleurone and starchy endosperm. In contrast, lipids (stained in orange-red by Sudan Red IV; Figure 1E, F) are mainly accumulated in the aleurone and in the embryo, as showed in longitudinally (Figure 1E) and transversally sectioned caryopses (Figure 1F).

Structure of the mature ovary

Rice ovaries were collected on a daily basis from anthesis to maturity, fixed in a modified formalin-acetic acid-alcohol (FAA) solution (Liu et al. 1993), dehydrated in an ethanol series, embedded in LR White resin, and sectioned to 1 μm in thickness before staining with periodic acid-Schiff (PAS) reagent and Coomassie Brilliant Blue (CBB). To define the fate of individual cell layers in the maternal tissue, attention was paid to three representative positions of transversely sectioned ovaries: The dorsal position where the primary vascular bundle is located, the upper lateral positions where two lateral vascular bundles are located, and the ventral position (Figure 2A, framed). A series of color codes was introduced to distinguish different tissues in the rice caryopsis (presented in Figure 2A) and is used throughout the remainder of this paper.

The pericarp in a mature rice ovary before anthesis consists of 11 to 12 layers of cells (Table 1). The outermost layer, the epicarp, consists of rectangular-shaped cells with thick walls (ec; Figure 2B–D). No starch grains were observed in these cells. The mesocarp tissue located underneath the epicarp has seven to eight layers of cells (mc; Figure 2B–D) and is characterized by the starch grain accumulation (stained red by PAS). Underneath the mesocarp, three layers of cytoplasm-dense endocarp cells (enc; Figure 2C, D) were recognizable in all locations except for the region near the dorsal vascular bundle. During caryopsis development (see below), two outer layers of endocarp cells form cross cells, while one inner layer forms tube cells. Under an electron microscope, we observed that cell walls between adjacent tube cells were thin and curly (indicated by red arrows; Figure 2E), which may allow these cells to be interlaced together.

A major vascular bundle, with well-formed tracheary elements (TEs; indicated by arrowheads; Figure 2B) and sieve elements (SEs; indicated by arrows; Figure 2B), was observed at the dorsal side of the mesocarp. Within this vascular bundle, many starch grain-free and cytoplasm-dense cells were recognizable (Figure 2B). In contrast, two minor vascular bundles located at the upper lateral positions were much smaller, with only a few TEs (indicated by arrowheads; Figure 2C) and SEs (indicated by arrows; Figure 2C). Within these three vascular bundles, SEs are always located on the outer side (near the epicarp), while TEs are located on the inner side (near the endosperm; Figure 2B, C). Based on their locations, we speculate that the dorsal vascular bundle originates from endocarp cells, while two lateral vascular bundles likely

originate from mesocarp cells. No vascular bundle was observed at the ventral side of the caryopsis (Figure 2D).

The tissue inside the endocarp consists of cytoplasm-dense, thin-walled integument cells. Both the outer (oi; Figure 2C, D) and the inner integument (ii; Figure 2C, D) have two cell layers. As can be seen from transversal sections, the outer integument extends from the dorsal to lateral side but does not enclose the inner integument and the nucellus, leaving a gap at the ventral side (indicated by arrowheads; Figure 2D). In contrast, the inner integument encloses the nucellus completely (Figure 2C, D). Transmission electron microscopy (TEM) revealed that cell walls formed between the inner integument and the nucellar epidermis were thickened and electron-dense (indicated by red arrowheads; Figure 2E, F). It has been proposed that cells located next to the dorsal vascular bundle provide a channel for water and nutrient loading toward the developing embryo and endosperm, based on dye-loading experiments (Krishnan and Dayanandan 2003).

The nucellus is located inside the inner integument and consists of an outer cell layer of nucellar epidermis (ne; Figure 2C, D) and 8 to 10 inner cell layers of highly vacuolated nucellar cells (nu; Figure 2B–D) to enclose the embryo sac inside.

Post-anthesis pericarp development

Although elongation of the ovary starts immediately after fertilization (Figure 1A), no evident expansion of epicarp cells was observed in transversely sectioned ovaries until 3 DAP (Figure 3C, C'). These cells occurred with the rapid elongation from 4 DAP onwards (Figure 4A, A') and reached their maximal sizes by 9 DAP (Figure 5C, C'). No starch grains were observed in epicarp cells at any point during the entire duration of caryopsis development. In contrast, mesocarp cells underneath were characterized by dynamic changes in starch grain accumulation (Figure 3A, A'). Number and size increases of starch grains were observed at 2 DAP (Figure 3B, B'); these starch grains reached the maximal number and size by 5 DAP (Figure 4B, B'). A gradual consumption of these starch grains occurred afterwards (Figure 4C, C'), and by 9 DAP very few starch grains remained (Figure 5C, C'). By 12 DAP, almost no starch grains could be detected (Figure 6A, A'). As with the epicarp cells, these mesocarp cells reached their maximal size at 9 DAP (Figure 5C, C'), and the degeneration of these cells occurred from 9 DAP onwards. A complete degeneration of these mesocarp cells was observed by 18 DAP (Figure 6B, B').

Endocarp cells were characterized by their small size and dense cytoplasm, with a small number of small starch grains in the first 4 DAP (Figures 3, 4A, A'). Differentiation of endocarp cells was observed from 5 DAP onwards, eventually producing two outer layers of tightly interlaced cross cells and one inner layer of loosely packed round-shaped tube cells by 9 DAP (Figures 4B', C', 5A'–C'), as illustrated in Figure 7. Cross cells (indicated by arrows; Figure 7A–E) are formed via elongation and expansion, while tube cells (indicated by arrowheads; Figure 7A–E) are formed in four steps (as illustrated in Figure 7F): (i) cell expansions in the first 2 DAP (Figure 7A, B); (ii) cell wall thickening from 2 to 5 DAP (Figure 7B, C); (iii) cell separations between neighboring tube cells from 5 to 6 DAP (Figure 7C, D); and (iv) cell shrinking from 6 to 9 DAP that form large intercellular spaces between adjacent tube cells
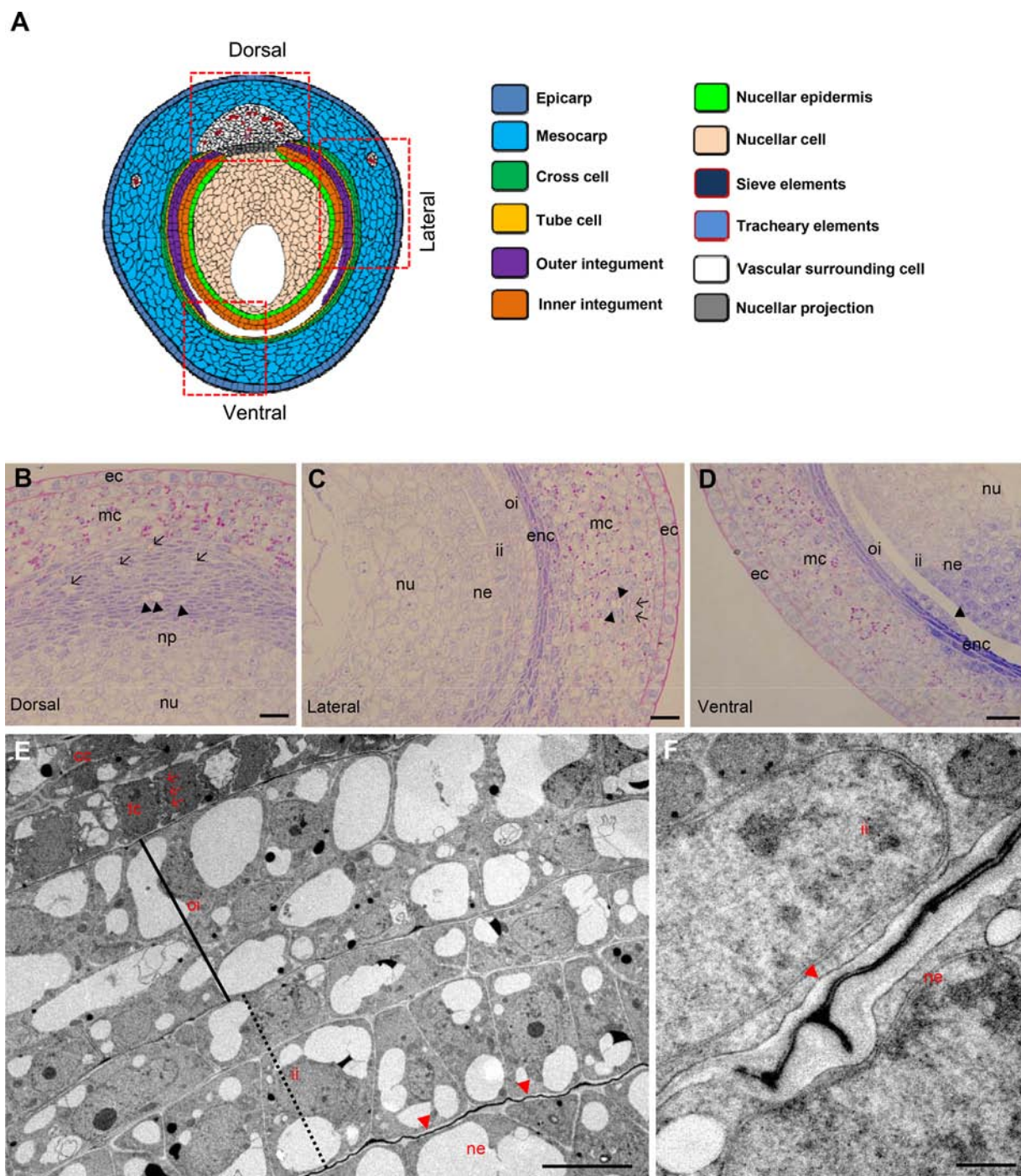
Figure 2. Structure of the mature rice ovary
(A) A graphic illustration of a transversely sectioned mature rice ovary immediately prior to fertilization. Different cell types are color-coded. The same color scheme is used throughout the manuscript. Dashed boxes indicate locations (dorsal, ventral and lateral) studied in detail in this work. **(B)** Structure of the rice ovary at the dorsal position. Arrowheads indicate tracheary elements (TEs), while arrows indicate sieve elements (SEs). **(C)** Structure of the rice ovary at the lateral position. Arrowheads indicate TEs, while arrows indicate SEs. **(D)** Structure of the rice ovary at the ventral position. Arrowheads indicate the end of the outer integument. **(E)** Ultrastructural observation of a mature rice ovary. Note the thickened and electron-dense cell walls formed between the inner integument (ii) and the nucellar epidermis (ne) (indicated by arrowheads). Arrows indicate the thin and curly cell walls formed between adjacent tube cells. The solid line indicates the outer integument (oi), while the dashed line indicates the inter integument (ii). **(F)** Thickened cell walls between the inner integument and nucellar epidermis. ec, epicarp; mc, mesocarp; enc, endocarp; np, nucellar projection; nu, nucellar; cc, cross cells; tc, tube cells; oi, outer integument; ii, inner integument; ne, nucellar epidermis. Scale bars = 20 μm **(B, C, D)**; 5 μm **(E)**; 500 nm **(F)**.

Table 1. Dynamic changes of cell layers in maternal tissues during rice caryopsis development

Tissue	Cell type	0 DAP	3 DAP	5 DAP	7 DAP	9 DAP	12 DAP	18 DAP	30 DAP
Pericarp	Epicarp	1	1	1	1	1	1	0	0
	Mesocarp	7–8	7–8	7–8	7–8	7–8	7–8	0	0
	Cross cell	2	2	2	2	2	2	2	0
	Tube cell	1	1	1	1	1	1	1	0
Testa	Outer integument	2	0	0	0	0	0	0	0
	Inner integument	2	2	2	2	2	1	0	0
	Nucellar epidermis	1	1	1	1	1	1	0	0
	Nucellar projection	4–5	4–5	4–5	4–5	4–5	4–5	4–5	0
	Nucellar cell	8–10	3–4	1–2	0	0	0	0	0

DAP, days after pollination

(Figure 7D, E). Note that cross cells and tube cells were not observed in the region near the dorsal vascular bundle (Figure 5A–C). It has been proposed that thick-wall tube cells may provide a rigid support to the caryopsis (Krishnan and Dayanandan 2003). Degeneration of tube cells and cross cells occurred simultaneously at 18 DAP (Figure 6B').

Post-anthesis vascular bundle development
As illustrated in Figure 2A, three vascular bundles are present in the mature ovary of rice. After anthesis, the number of SEs (a region indicated by black dashed line) and TEs (a region indicated by red dashed line) in the dorsal vascular bundle increased rapidly (Figures 3A–C, 4A–C, 5A–C), reaching the maximal number by 8 DAP (Figure 5B). During this period, new SEs were formed in clusters from neighboring parenchyma cells, producing six to eight SE clusters, with 30 to 40 SEs in total at the end (Figure 5B). Similarly, the formation of new TEs also occurred immediately after fertilization (Figures 3A–C, 4A–C, 5A–C), and reached their final forms with 15 to 20 TEs in total (Figure 5B). These SEs and TEs were morphologically intact until 18 DAP (Figures 5B, C, 6A, B), and started to degenerate thereafter. By 27 DAP, most SEs and TEs in the dorsal vascular bundle were collapsed (Figure 6D). The cytoplasm-dense parenchyma cells were also degenerated at the same time (Figure 6D).

In contrast, not much increase in numbers of TEs and SEs was observed in two lateral vascular bundles (indicated by blue dashed line) after anthesis (Figures 3A'–C', 4A'–C', 5A'–C'). By 9 DAP, three to five SEs were recognizable in each bundle, with hardly any TEs detected (Figure 5C'), suggesting these lateral vascular bundles play a minor role in the delivery of nutrients and water. By 21 DAP, both the TEs and the SEs in these two lateral vascular bundles were collapsed, and the parenchyma cells inside these vascular bundles were degenerated as well (Figure 6C').

Post-anthesis integument development
The outer integument in the rice caryopsis disappeared completely by 3 DAP (Figure 3C'), allowing the inner integument to contact directly the endocarp. Cells of the outer layer of the inner integument degenerated by 7 DAP (Figure 5A'), while the inner layer of the inner integument remained alive for a much longer period and degenerated by 18 DAP (Figure 6B'). Thickened cell walls, stained dark-red by

PAS, were formed between the inner integument and the nucellar epidermis from 8 to 12 DAP (Figures 5B', C', 6A').

Post-anthesis nucellar development
At the time of anthesis, the nucellus in the rice caryopsis has 8 to 10 cell layers (Table 1; Figure 2C). The degeneration of these cells occurred rapidly from 2 DAP onwards, and started from the innermost layer and proceeded to outer layers (indicated by asterisks; Figure 3B, B'). By 3 DAP, only four cell layers were left, with one layer of nucellar epidermis and three layers of nucellar tissue (Figure 3C, C'). By 5 DAP, only two layers of nucellar cells were observed (Figure 4B, B'). By 6 DAP, all nucellar tissues, except for the nucellar epidermis and nucellar projection, were degenerated (Figure 4C, C').

The nucellar epidermis is a specialized tissue in the caryopsis with thickened cell walls at its outer surfaces. From 1 to 6 DAP, cells in the nucellar epidermis were square in shape (Figures 3, 4), but changed to a rectangular shape by 7 DAP (Figure 5A'). Some starch grains were observed in nucellar epidermal cells between 2 and 4 DAP (Figures 3B', C', 4A'). The degeneration of the nucellar epidermis started from 12 DAP onwards, characterized by a gradual loss of cytoplasm (Figure 6A'). Complete degeneration of nucellar epidermis cells was observed by 18 DAP (indicated by blue arrowheads; Figure 6B'). We noted that a small cluster of nucellar cells located next to the dorsal vascular bundle, named the nucellar projection, remained alive until 21 DAP (Figure 6C). No thick-walled nucellar epidermal cells were observed in this region.

DISCUSSION

Post-fertilization caryopsis development of rice occurs in a protected environment enclosed by the palea and the lemma (Itoh et al. 2005). Although studies carried out in the past have provided substantial knowledge about the rice caryopsis (Zee 1972; Gu et al. 2002; Evers and Millar 2002; Krishnan and Dayanandan 2003), a complete picture of cellular changes in the rice caryopsis remains lacking. In this study, cytohisto-logical analyses were performed in maternal tissues of the rice caryopsis on a daily basis throughout the entire course of caryopsis development, which allowed us to identify dynamic changes in cell expansion, cell wall thickening, and starch grain accumulation. More strikingly, a series of well-defined cell degenerations were observed in these tissues.
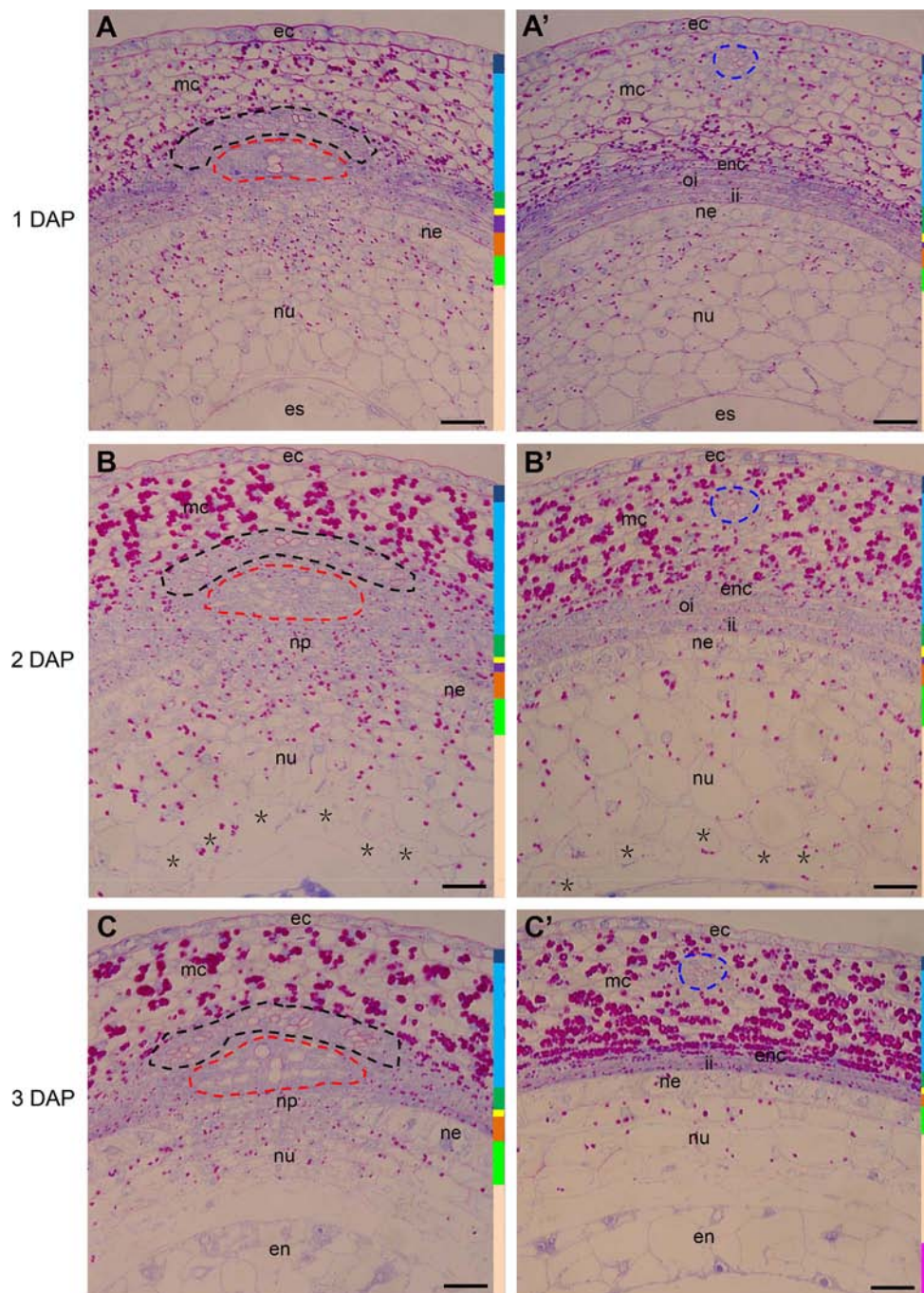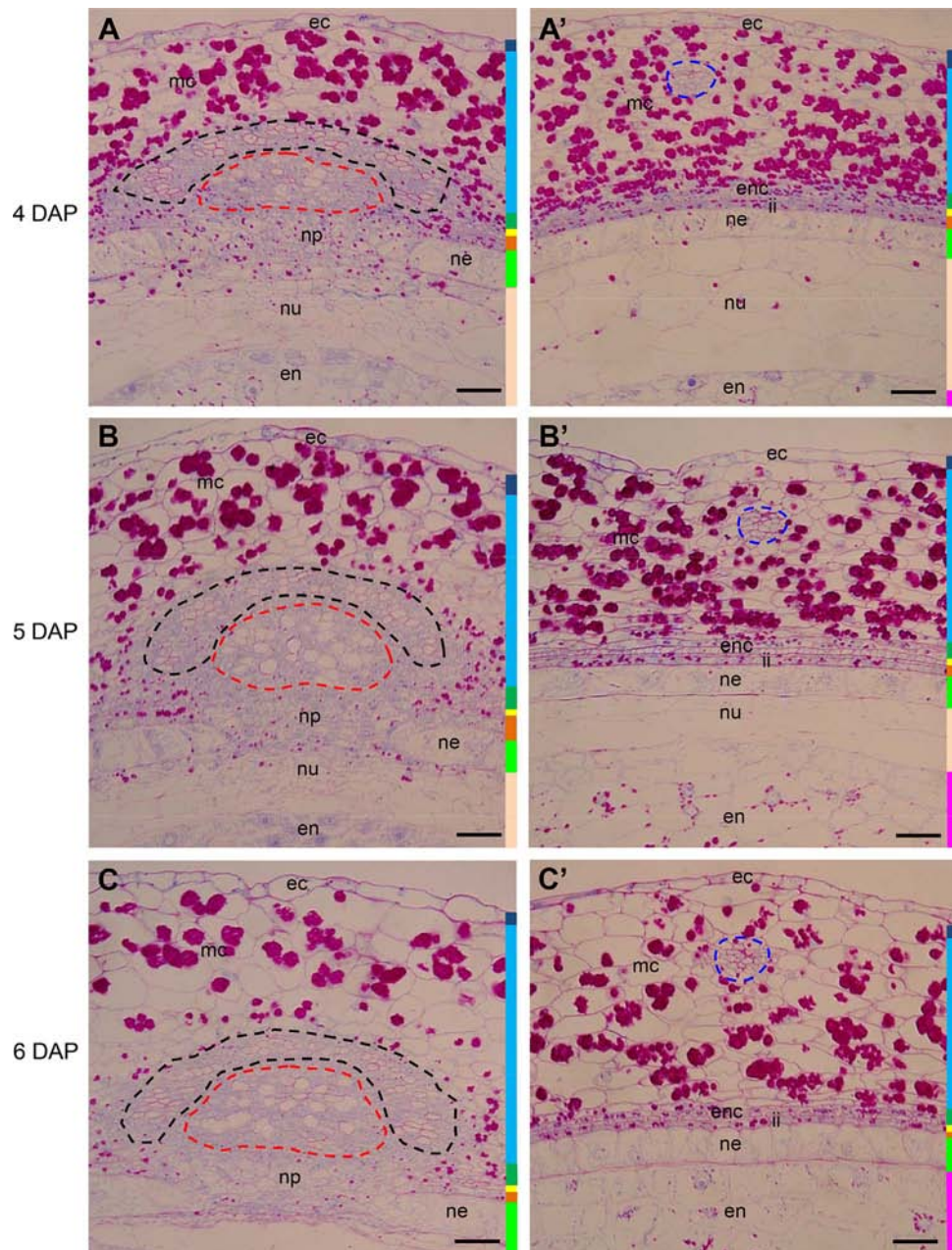
Figure 3. Morphological changes in rice caryopsis from 1 to 3 days after pollination (DAP)
Transversely sectioned maternal tissues at the dorsal (**A–C**) and lateral positions (**A'−C'**) at 1 (**A, A'**), 2 (**B, B'**), and 3 DAP (**C, C'**). Red dashed line indicates TEs, while black dashed line indicates SEs. Blue dashed line indicates the lateral vascular bundle. Asterisks indicate degenerating nucellar cells. ec, epicarp; mc, mesocarp; enc, endocarp; np, nucellar projection; nu, nucellar; cc, cross cell; tc, tube cell; oi, outer integument; ii, inner integument; ne, nucellar epidermis; es, embryo sac. Scale bars = 20 μm.

Dynamic changes of maternal tissues in rice caryopsis
The maternal tissues of the rice caryopsis contain nine distinct cell types (Figure 8): four in the pericarp (epicarp, mesocarp, cross cell and tube cell) and five in the testa (outer integument, inner integument, nucellar projection, nucellar epidermis and nucellar cell). One interesting phenomenon observed in this study is the degeneration of these cell types at discrete time points, as illustrated in Table 1 and Figure 8. The first tissue in the caryopsis that underwent degeneration after anthesis is the outer integument, started at 2 DAP and

Figure 4. Morphological changes in rice caryopsis from 4 to 6 days after pollination (DAP)
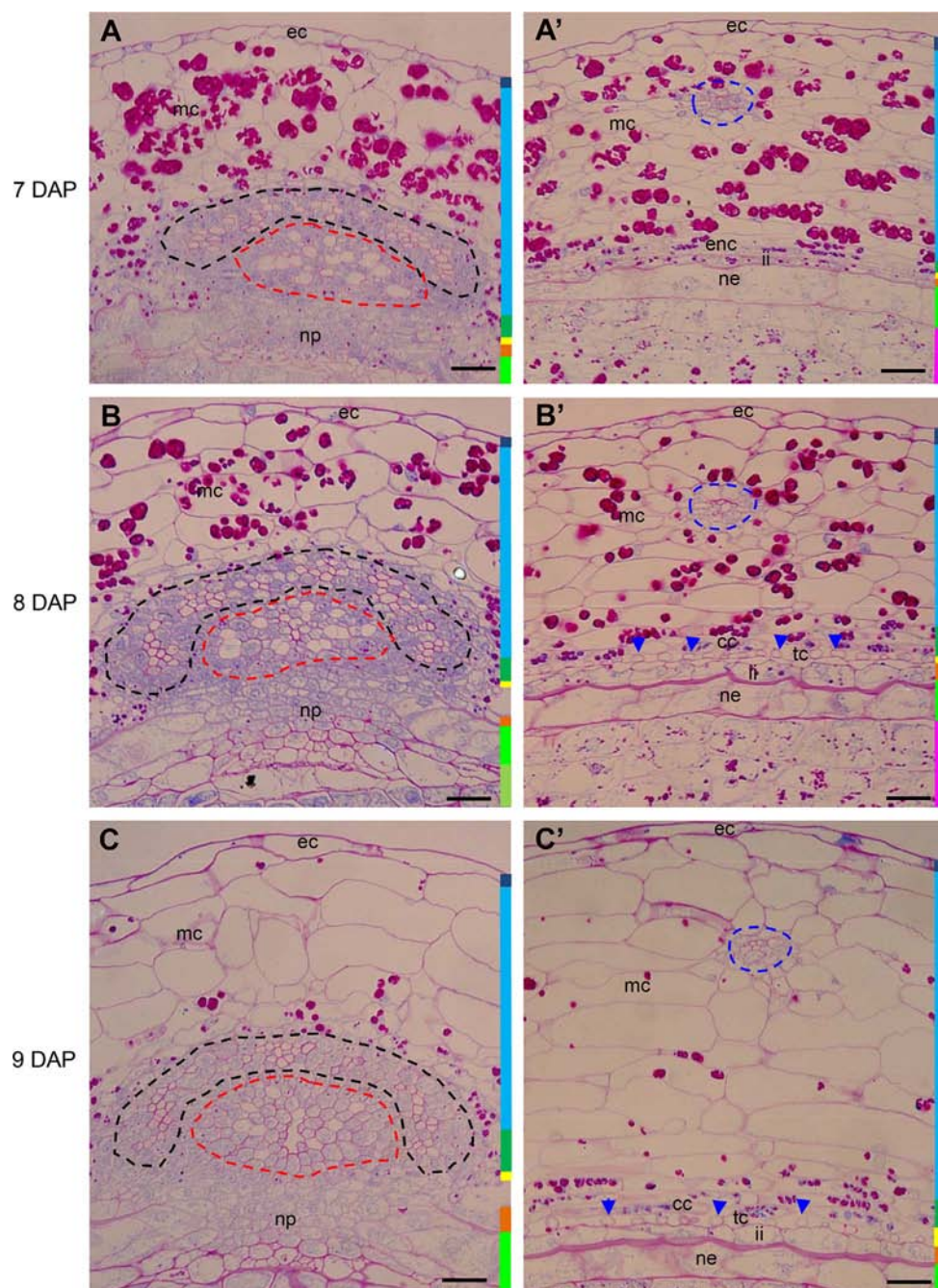Transversely sectioned maternal tissues at the dorsal **(A–C)** and lateral positions **(A'–C')** at 4 **(A, A')**, 5 **(B, B')**, and 6 DAP **(C, C')**. Red dashed line indicates TEs, while black dashed line indicates SEs. Blue dashed line indicates the lateral vascular bundle. ec, epicarp; mc, mesocarp; enc, endocarp; np, nucellar projection; nu, nucellar; ii, inner integument; ne, nucellar epidermis; en, endosperm. Scale bars = 20 μm.

disappeared completely by 3 DAP. In parallel, the degeneration of nucellar cells starts at the same time, and by 3 DAP the number of cell layers has decreased from 8 to 10, to 4; by 5 DAP, all nucellar tissues except for the nucellar epidermis and the nucellar projection had degenerated. One major degeneration point is observed at 18 DAP, by which point all of the cells of the epicarp, mesocarp, endocarp, integument and nucellar tissue have degenerated. Although the degeneration of several cell layers has been noted in cereal grains previously (Krishnan and Dayanandan 2003; Radchuk et al. 2009; Radchuk et al. 2011), this study provides a complete atlas of the degeneration of all maternal tissues in the rice caryopsis (Figure 9).

The analysis of whole genome microarray identified several seed-specific transcription factors in MYB, NAM and MADS-box gene families, and some of them have been showed to be essential for the rice caryopsis development (Wang et al. 2010; Sharma et al. 2012). Recent studies have shown that the
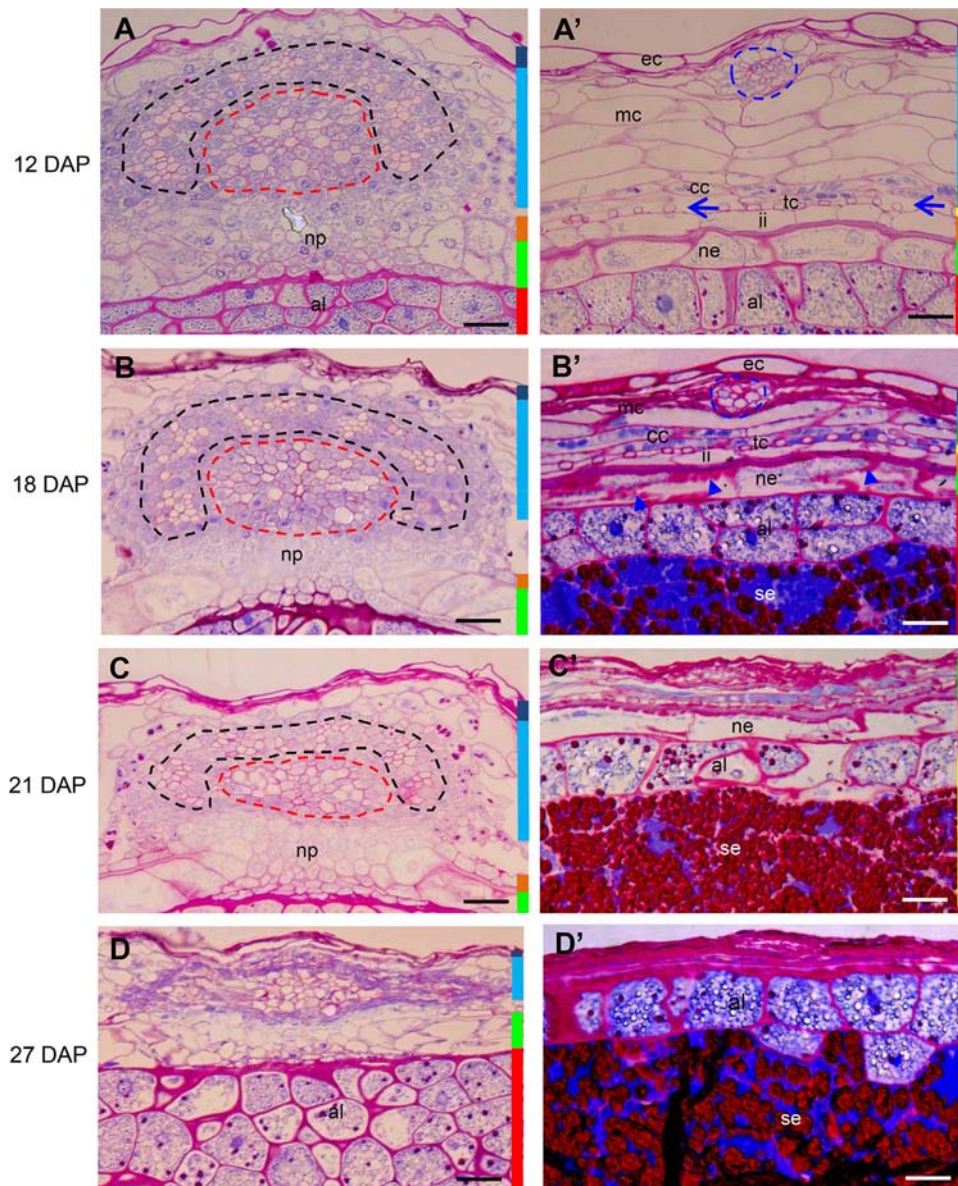
Figure 5. Morphological changes in rice caryopsis from 7 to 9 days after pollination (DAP)
Transversely sectioned maternal tissues at the dorsal **(A–C)** and lateral positions **(A'–C')** at 7 **(A, A')**, 8 **(B, B')** and 9 DAP **(C, C')**. Red dashed line indicates TEs, while black dashed line indicates SEs. Blue dashed line indicates the lateral vascular bundle. Blue arrowheads indicate tube cells. ec, epicarp; mc, mesocarp; np, nucellar projection; cc, cross cell; tc, tube cell; ii, inner integument; ne, nucellar epidermis. Scale bars = 20 μm.

transcription factor OsMADS29 negatively regulates the degenerations of the nucellus and nucellar projection, as suppressed *OsMADS29* expression results in delayed degradation of these two tissues and defective grain filling (Yin and Xue 2012; Yang et al. 2012). In agreement with this finding, we observed that, although the nucellus starts to degenerate from 2 DAP, the nucellar projection is not fully degenerated until 21

DAP, a point by which grain filling is already completed. Thus, in wildtype rice plants, it is unlikely that effective nutrient loading can occur after 21 DAP, since most maternal tissues including the dorsal vascular bundle have degenerated by that point. Another study showed that *OsMADS29* is expressed most abundantly in the dorsal vascular bundle, the aleurone layer and the embryo, suggesting that *OsMADS29* may regulate embryo and

Figure 6. Morphological changes in rice caryopsis from 12 to 27 days after pollination (DAP)
Transversely sectioned maternal tissues at the dorsal **(A-D)** and lateral positions **(A'-D')** at 12 **(A, A')**, 18 **(B, B')**, 21 **(C, C')** and 27 DAP **(D, D')**. Red dashed line indicates TEs, while black dashed line indicates SEs. Blue dashed line indicates the lateral vascular bundle. Blue arrows indicate tube cells. Blue arrowheads indicate cell wall protrusions in the nucellar epidermis. ec, epicarp; mc, mesocarp; np, nucellar projection; cc, cross cell; tc, tube cell; ne, nucellar epidermis, al, aleurone; se, starchy endosperm. Scale bars = 20 μm.

endosperm development by affecting hormone homeostasis (Nayar et al. 2013). In barley, it has been shown that the programmed cell death (PCD) events of the maternal caryopsis tissues coincide with endosperm development and the spatial and temporal elevations of some caspase-like activities in maternal tissues (Radchuk et al. 2011; Tran et al. 2014). Although the ultimate physiological role of these rapid degenerations of maternal tissues is not yet known, it is plausible that the timely degeneration of these tissues may facilitate effective nutrient loading and may enable the starch accumulated in maternal tissues to be re-utilized for embryo and endosperm

development. Further studies are needed to elucidate how these cell layer-specific degenerations are regulated, and which ones, if any, of these degenerations are necessary for grain filling.

Roles of maternal tissues in grain filling
It is widely assumed that caryopsis development relies heavily on coordinated interaction between maternal and filial tissues. Maternal tissues likely play at least two major roles in grain filling: (i) to accommodate the developing embryo and endosperm; and (ii) to deliver water and nutrients to the
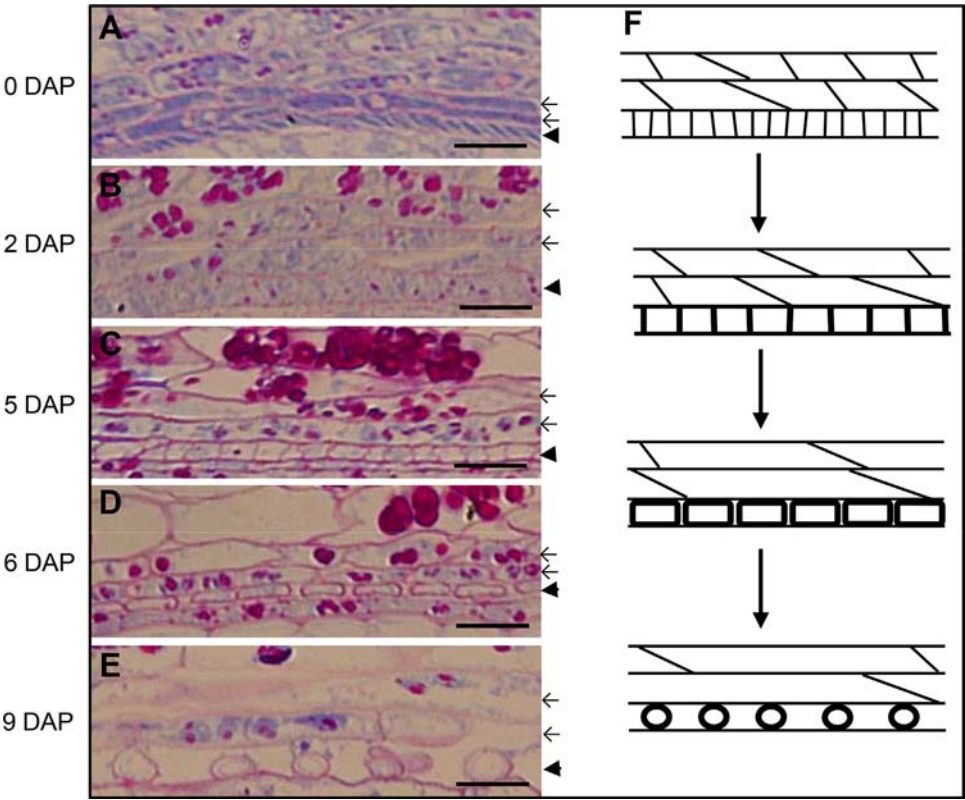
Figure 7. Differentiation of cross cells and tube cells
The morphology of cross cells and tube cells at 0 **(A)**, 2 **(B)**, 5 **(C)**, 6 **(D)** and 10 days after pollination (DAP) **(E)**. Two arrows at the side of each picture indicate cross cell layers, while the arrowhead indicates tube cell layer. **(F)** Graphical representation showing the differentiation of tube cells occurring from 0 **(A)** to 9 DAP **(E)**, and the elongation and expansion of cross cells. Note that shrinking of tube cells from 6 to 9 DAP generates large spaces between adjacent tube cells. Scale bars = 20 μm.

developing embryo and endosperm. Dynamic changes observed in this study in maternal tissues during caryopsis development seem to correlate with the fulfillment of these two major roles. After fertilization (0–9 DAP), the rice caryopsis undergoes the rapid expansion in three dimensions. The changes of cell shape and the thickening of cell wall in the maternal tissues coordinate with the expansions of caryopsis for accommodating the developing filial tissues. Detailed microarray profiling using the 25 stages/organs of rice

reproductive development showed that many putative pectin methylesterases and putative cellulose synthase genes related to cell wall component metabolism expressed in embryogenesis stages, suggesting cell wall metabolism, is probably essential for developing seeds (Fujita et al. 2010). From 5 to 9 DAP, two tightly interlaced cross cell layers and one loosely packed tube cell layer are formed in the endocarp; this may provide rigid support to the developing caryopsis. It is believed that the dorsal vascular bundle plays a crucial role
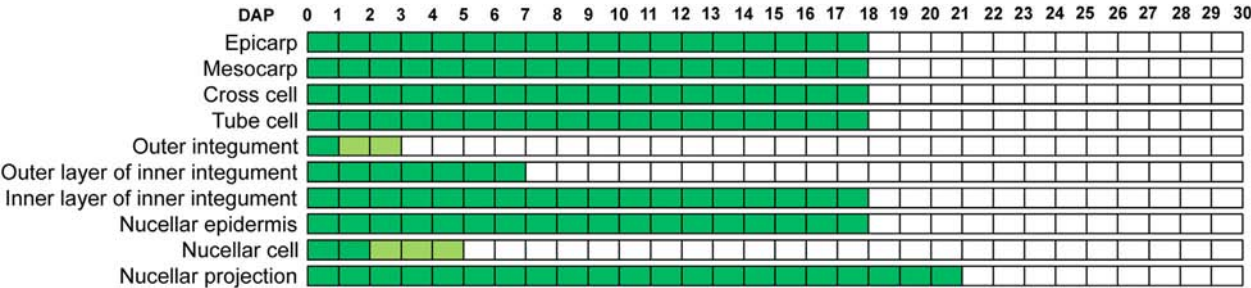
Figure 8. Degeneration of various maternal tissues in rice caryopsis at different time points
Each box represents 1 day. Boxes filled with dark green indicate cells that are alive, boxes filled with pale green indicate cells undergoing gradual degeneration, and empty boxes represent cells that are completely degenerated.
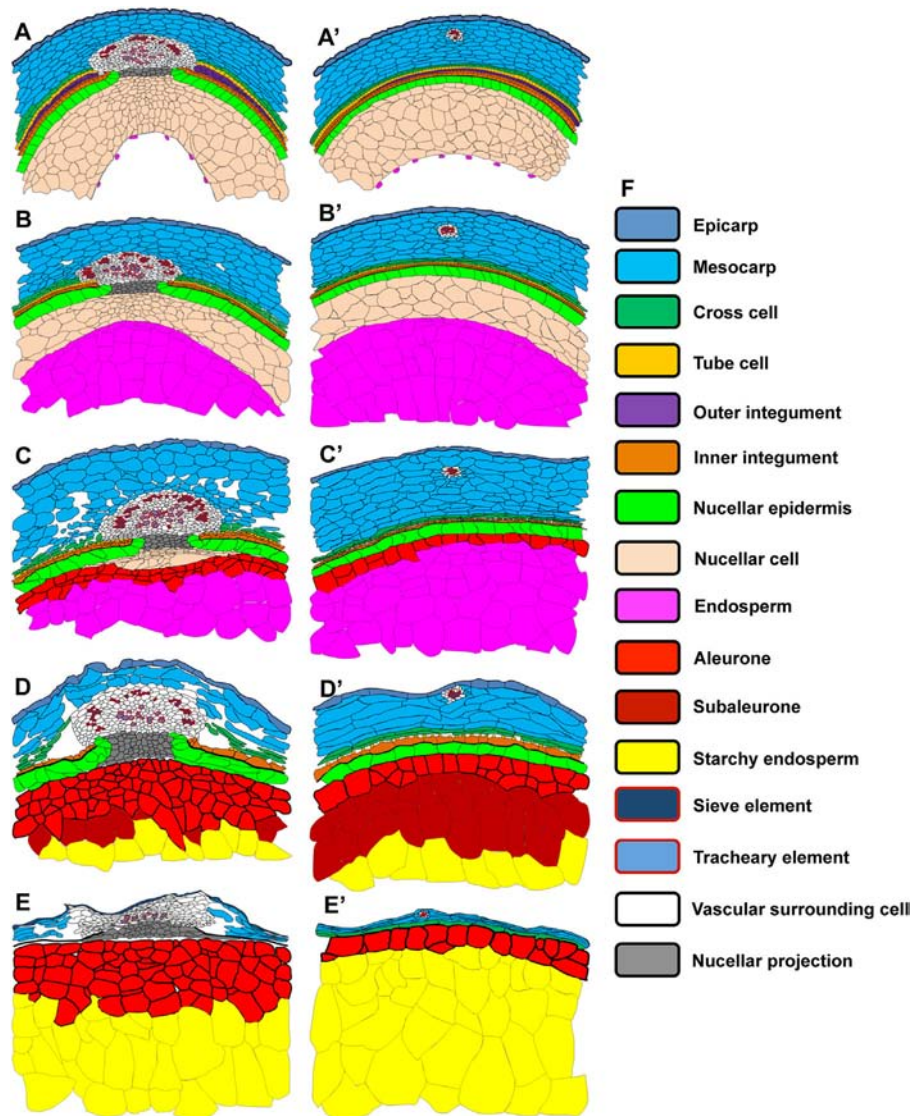
Figure 9. Schematic illustrations of the dynamic changes in individual maternal cell layers during rice caryopsis development
Morphologies of different maternal and endosperm tissues at 2 days after pollination (DAP) **(A, A')**, 3 to 5 DAP **(B, B')**, 6 to 9 DAP **(C, C')**, 10 to 18 DAP **(D, D')** and 19 to 30 DAP **(E, E')** at the dorsal **(A–D)** and lateral positions **(A'–D')**. Individual cell layers are color-coded as shown in **(F)**.

in loading water and photosynthesis assimilates to the developing endosperm (Oparka and Gates 1981, 1982; Krishnan and Dayanandan 2003; Radchuk et al. 2011; Yang et al. 2012). In this study, we observed rapid establishment of TEs and SEs in the dorsal vascular bundle in the first 6 DAP. Formation of these TEs and SEs correlated tightly with the rapid accumulation of starch grains in the starchy endosperm, which occurs between 5 and 18 DAP. By 8 DAP, thickened cell walls were formed between the inner integument and the nucellar epidermis in all regions surrounding the embryo sac, with the exception of the nucellar projection. These fortified cell walls at the outer surface of the nucellar epidermis are rich in lipids, a situation that resembles the cuticle layer in the epidermis and may help to establish a waterproof barrier that isolates the developing endosperm (Oparka and Gates 1981;

Ellis and Chaffey 1987; Krishnan and Dayanandan 2003). In contrast, the lack of a nucellar epidermis in the region near the dorsal vascular bundle may help to establish an open channel for loading water and nutrients to the developing endosperm and embryo (Krishnan and Dayanandan 2003). In barley and wheat, it has been shown that the dorsal vascular bundle is the major route for water and nutrient deliveries to the developing caryopsis (Felker and Shannon 1980; Wang and Fisher 1994a, 1994b; Zhang et al. 2007). In rice it has been shown that the cell wall invertase *GIF1* is expressed in the dorsal vascular bundle (Wang et al. 2008a), and *Monosaccharide Transporter 4* (*MST4*) are expressed in both the maternal tissues, including the vascular bundle and filial tissues (Wang et al. 2007), suggesting the presence of one route delivery of fructose and glucose to starchy endosperm after the sucrose

is released from the dorsal vascular bundle. We showed recently that a NF-YB1 transcription factor expressed in aleurone regulates the expressions of three sucrose transporters in the aleurone, allowing sucrose to be loaded directly to the starchy endosperm of rice (Bai et al. 2015), suggesting the presence of another independent route for loading sugars to the rice endosperm. Physiological studies using radioactive labeled sugars performed in the past have already showed that sucrose is the major form for sugar loaded to the barley endosperm (Melkus et al. 2011). As illustrated in Figure 10, the formation of a nucellar epidermis-dorsal vascular bundle-nucellar projection complex may establish a cellular channel to allow efficient water and sugar to be delivered from the dorsal vascular bundle to the developing caryopsis in a regulated manner.

Another interesting observation is that, in the first 6 days of caryopsis development, a large number of starch grains accumulated in mesocarp cells, followed by a rapid consumption of these starch grains from 7 to 9 DAP. This type of transient starch accumulation has also been observed in maternal tissues of barley and wheat (Radchuk et al. 2009; Xiong et al. 2013). Although the physiological significance of these starch grains has not been characterized, it is reasonable to assume that they are degraded and re-utilized for grain filling.

In summary, we here show that the post-fertilization development of the rice caryopsis involves synergetic differentiation and degeneration of various maternal tissues. These dynamic changes may facilitate water and nutrient delivery to the developing embryo and endosperm for grain filling, leading eventually to the formation of a functional seed. Detailed molecular genetic studies in this area in the future should facilitate our understanding of grain production in cereal crops in general.

MATERIALS AND METHODS

Plant Materials
Rice plants (*Oryza sativa* L. ssp. *japonica*, cultivar Zhonghua 11) were grown in a net-protected experimental field at the Institute of Botany, the Chinese Academy of Sciences (Beijing, China). Spikelets were marked on the surface of the hull to denote flowering dates and were then sampled daily throughout the 30-day period of caryopsis development.

Microscopy
For staining of lipids, mature rice caryopses were longitudinally or transversally sectioned using a razor blade and then stained in 0.5% Sudan IV (Brundrett et al. 1991) for 24 h at room temperature. For staining of starch, hand-sectioned caryopses were stained in Lugo (Sigma) for 5 min before being washed with distilled water and observed and imaged under a dissection microscope (Nikon, SMZ800). For semi-thin sections, rice grains were collected at different DAP and caryopses were isolated after removing the palea and lemma; these were then hand-sectioned transversely into 2 mm slices using a razor blade, embedded in LR White resin and cytohistologically analyzed as described previously (Schnelder 1981; Yu et al. 2012), except for counter-staining with 0.1% CBB for 20 min. Pictures were taken under a microscope (Eclipse 80i, Nikon, Japan). For transmission electron microscopy, sliced caryopses were fixed in 2.5% glutaraldehyde in a 0.1 mol/L sodium phosphate buffer
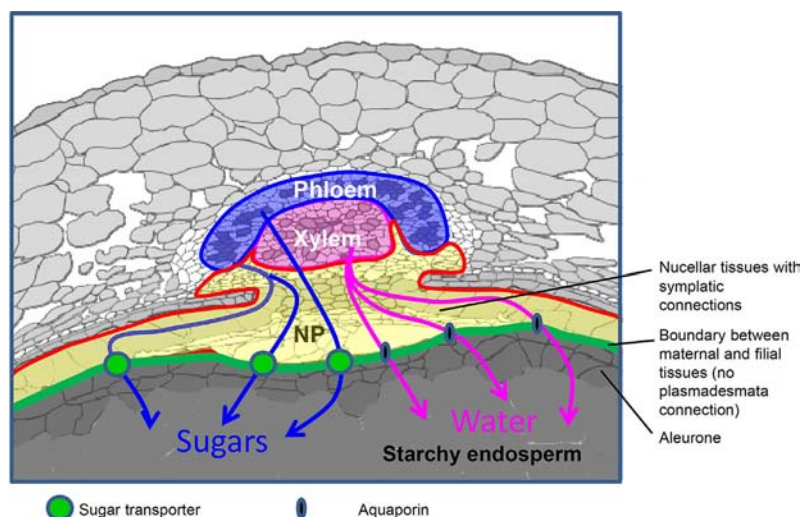
Figure 10. A diagrammatic representation of a possible route for water and nutrient loading from the dorsal vascular bundle to the developing endosperm
This drawing was made based on morphological observations from this study as well as previously published studies (Oparka and Gates 1981; Krishnan and Dayanandan 2003). Since extensive plasmadesmata connections are present between parenchyma cells in the vascular bundle and the nucellar projection, it is assumed that sugars and water can pass through these cells symplasmically. However, since there are no plasmadesmata connections at the maternal and filial interface (between the nucellar projection and the aleurone), it is assumed that sugar transporters and/or aquaporins are involved in delivering nutrients and water to the developing endosperm in an apoplastic manner.

(pH 7.0) for 1 h, washed in the same buffer on an orbital shaker three times for 30 min each time, and then post-fixed in 1% osmium tetraoxide at 4 °C overnight before being embedded in Spurr resin, sectioned, stained and observed under a JEOL-1230 transmission electron microscope, as reported previously (Roland and Vian, 1991).

ACKNOWLEDGEMENTS

AUTHOR CONTRIBUTIONS

X.W. and D.L. designed and performed the experiments. J.L. and C.-M.L. analyzed the data and wrote the manuscript.

REFERENCES

Bai AN, Lu XD, Li DQ, Liu JX, Liu CM (2015) NF-YB1-regulated expression of sucrose transporters in aleurone facilitates sugar loading to rice endosperm. **Cell Res** doi: 10.1038/cr.2015.116

Becraft PW, Yi G (2011) Regulation of aleurone development in cereal grains. **J Exp Bot** 62: 1669–1675

Bosnes M, Weideman F, Olsen OA (1992) Endosperm differentiation in barley wild-type and sex mutants. **Plant J** 2: 661–674

Brundrett MC, Kendrick B, Peterson CA (1991) Efficient lipid staining in plant material with Sudan Red 7B or Fluoral Yellow 088 in polyethylene glycol-glycerol. **Biotech Histochem** 66: 111–116

Ellis JR, Chaffey NJ (1987) Structural differentiation of the nucellar epidermis in the caryopsis of rice. **Ann Bot** 60: 671–675

Evers T, Millar S (2002) Cereal grain structure and development: Some implications for quality. **J Cereal Sci** 36: 261–284

Felker FC, Shannon JC (1980) Movement of ^{14}C-labelled assimilates into kernels of *Zea mays* L. Anatomical examination and microautoradio graphic study of assimilate transfer. **Plant Physiol** 65: 864–870

Fujita M, Horiuchi Y, Ueda Y, Mizuta Y, Kubo T, Yano K, Yamaki S, Tsuda K, Nagata T, Niihama M, kato H, Kikuchi S, Hamada K, Mochizuki T, Ishimizu T, Iwai H, Tsutsumi N, Kurata N (2010) Rice expression atlas in reproductive development. **Plant Cell Phyisol** 51: 2060–2081

Goff SA, Ricke D, Lan TH, Presting G, Wang R, Dunn M, Glazebrook J, Sessions A, Oeller P, Varma H, Hadley D, Hutchison D, Martin C, Katagiri F, Lange BM, Moughamer T, Xia Y, Budworth P, Zhong J, Miguel T, Paszkowski U, Zhang S, Colbert M, Sun WL, Chen L, Cooper B, Park S, Wood TC, Mao L, Quail P, Wing R, Dean R, Yu Y, Zharkikh A, Shen R, Sahasrabudhe S, Thomas A, Cannings R, Gutin A, Pruss D, Reid J, Tavtigian S, Mitchell J, Eldredge G, Scholl T, Miller RM, Bhatnagar S, Adey N, Rubano T, Tusneem N, Robinson R, Feldhaus J, Macalma T, Oliphant A, Briggs S (2002) A draft sequence of the rice genome (*Oryza sativa* L. ssp. japonica). **Science** 296: 92–100

Gu YJ, Wang Z, Chen J, Zhao GY (2002) The structure and function of pericarp in rice. **Acta Agron Sinica** 28: 439–444

Itoh JI, Nonomura KI, Ikeda K, Yamaki S, Inukai Y, Yamagishi H, Kitano H, Nagato Y (2005) Rice plant development: From zygote to spikelet. **Plant Cell Physiol** 46: 23–47

Jones TJ, Rost TL (1989) Histochemistry and ultrastructure of rice (*Oryza sativa*) zygotic embryogenesis. **Am J Bot** 76: 504–520

Krishnan S, Dayanandan P (2003) Structural and histochemical studies on grain-filling in the caryopsis of rice (*Oryza sativa* L.). **J Bio Sci** 28: 455–469

Liu CM, Xu ZH, Chua NH (1993) Auxin polar transport is essential for the establishment of bilateral symmetry during early plant embryogenesis. **Plant Cell** 5: 621–630

Lopes MA, Larkins BA (1993) Endosperm origin, development, and function. **Plant Cell** 5: 1383–1399

Melkus G, Rolletschek H, Fuchs J, Radchuk V, Grafahrend-Belau E, Sreenivasulu N, Rutten T, Weier D, Heinzel N, Schreiber F, Altmann T, Jakob PM, Borisjuk L (2011) Dynamic ^{13}C/^{1}H NMR imaging uncovers sugar allocation in the living seed. **Plant Biotechnol J** 9: 1022–1037

Nayar S, Sharma R, Tyagi AK, Kapoor S (2013) Functional delineation of rice MADS29 reveals its role in embryo and endosperm development by affecting hormone homeostasis. **J Exp Bot** 64: 4239–4253

Opanowicz M, Hands P, Betts D, Parker ML, Toole GA, Mills ENC, Doonan JH, Drea S (2011) Endosperm development in *Brachypodium distachyon*. **J Exp Bot** 62: 735–748

Oparka KJ, Gates P (1981) Transport of assimilates in the developing caryopsis of rice (*Oryza sativa* L.): Ultrastructure of the pericarp vascular bundle and its connection with the aleurone layers. **Planta** 151: 561–573

Oparka KJ, Gates P (1982) Ultrastructure of the developing pigment strand of rice (*Oryza sativa* L.) in relation to its role in solute transport. **Protoplasma** 113: 33–43

Radchuk V, Borisjuk L, Sreenivasulu N, Merx K, Mock H-P, Rolletschek H, Wobus U, Weschke W (2009) Spatiotemporal profiling of starch biosynthesis and degradation in the development barley grain. **Plant Physiol** 150: 190–204

Radchuk V, Weier D, Radchuk R, Weschke W, Weber H (2011) Development of maternal seed tissue in barley is mediated by regulated cell expansion and cell disintegration and coordinated with endosperm growth. **J Exp Bot** 62: 1217–1227

Roland JC, Vian B (1991) General preparation and staining of thin sections. In: Hall JL, Hawes C, eds. *Electron Microscopy of Plant Cells*. Academic press, London. pp. 1–66

Sang T, Ge S (2013) Understanding rice domestication and implications for cultivar improvement. **Curr Opin Plant Biol** 16: 139–46

Saulnier L, Guillon F, Chateigner-Boutin AL (2012) Cell wall deposition and metabolism in wheat grain. **J Cereal Sci** 56: 91–108

Schnelder H (1981) Plant anatomy and general botany. In: G. Clark, ed. *The Staining Procedures*, 4th ed. Williams & Wilkins, Baltimore. pp. 315–333

Sharma R, Agarwal P, Ray S, Deveshwar P, Sharma P, Sharma N, Nijhawan A, Jain M, Singh Ak, Singh VP, Khurana JP, Tyagi AK, Kapoor S (2012) Expression dynamics of metabolic and regulatory components across stages of panicle and seed development in *indica* rice. **Funct Integr Genomics** 12: 229–248

Tran V, Weier D, Radchuk R, Thiel J, Radchuk V (2014) Caspase-like activities accompany programmed cell death events in developing barley grains. **PLoS ONE** 10: e109426

Wang ET, Wang JJ, Zhu XD, Hao W, Wang LY, Lin Q, Zhang LX, He W, Lu BR, Lin HX, Ma H, Zhang GQ, He ZH (2008a) Control of rice grain-filling and yield by a gene with a potential signature of domestication. **Nat Genet** 40: 1370–1374

Wang L, Xie WB, Chen Y, Tang WJ, Yang JY, Ye JY, Liu L, Lin YJ, Xu CG, Xiao JH, Zhang QF (2010) A dynamic gene expression atlas covering the entire life cycle of rice. **Plant J** 61: 752–766

Wang YQ, Xu HL, Wei XL, Chai CL, Xiao YG, Zhang Y, Chen B, Xiao GF, Ouwerkerk PBF, Wang M, Zhu Z (2007) Molecular cloning and expression analysis of a monosaccharide transporter gene OsMST4 from rice (*Oryza sativa* L.) **Plant Mol Bio** 65: 439–451

Wang YQ, Wei XL, Xu HL, Chai CL, Meng K, Zhai HL, Sun YG, Wu B, Xiao GF, Zhu Z (2008b) Cell-wall invertases from rice are differentially expressed in caryopsis during the grain filling stage. **J Integr Plant Biol** 50: 466–474

Wang N, Fisher DB (1994a) Monitoring phloem unloading and post-phloem transport by microperfusion of attached wheat grains. **Plant Physiol** 104: 7–17

Wang N, Fisher DB (1994b) The use of fluorescent tracers to characterize the post-phloem transport pathway in maternal tissue of developing wheat grains. **Plant Physiol** 104: 17–27

Wang Z, Gu YJ, Zheng YK, Wang HH (2012) Ultrastructure observation of rice endosperm cell development and its mineral element analysis. **Chin J Rice Sci** 26: 693–705

Xiong F, Yu XR, Zhou L, Wang F, Xiong AS (2013) Structural and physiological characterization during wheat pericarp development. **Plant Cell Rep** 32: 1309–1320

Yang X, Wu F, Lin X, Du X, Chong K, Gramzow L, Schilling S, Becker A, Theissen G, Meng Z (2012) Live and let die—the B*sister* MADS-box gene *OsMADS29* controls the degeneration of cells in maternal tissues during seed development of rice (*Oryza sativa*). **PLoS ONE** 7: e51435

Yin LL, Xue HW (2012) The MADS29 transcription factor regulates the degradation of the nucellus and the nucellar projection during rice seed development. **Plant Cell** 24: 1049–1065

Yoshida H, Nagato Y (2011) Flower development in rice. **J Exp Bot** 62: 4719–4730

Yu DL, Jiang L, Gong HQ, Liu CM (2012) *EMBRYONIC FACTOR 19* encodes a PPR protein that is essential for the initiation of zygotic embryogenesis in *Arabidopsis*. **J Integr Plant Biol** 54: 55–64

Yu J, Hu S, Wang J, Wong GK, Li S, Liu B, Deng Y, Dai L, Zhou Y, Zhang X, Cao M, Liu J, Sun J, Tang J, Chen Y, Huang X, Lin W, Ye C, Tong W, Cong L, Geng J, Han Y, Li L, Li W, Hu G, Huang X, Li W, Li J, Liu Z, Li L, Liu J, Qi Q, Liu J, Li L, Li T, Wang X, Lu H, Wu T, Zhu M, Ni P, Han H, Dong W, Ren X, Feng X, Cui P, Li X, Wang H, Xu X, Zhai W, Xu Z, Zhang J, He S, Zhang J, Xu J, Zhang K, Zheng X, Dong J, Zeng W, Tao L, Ye J, Tan J, Ren X, Chen X, He J, Liu D, Tian W, Tian C, Xia H, Bao Q, Li G, Gao H, Cao T, Wang J, Zhao W, Li P, Chen W, Wang X, Zhang Y, Hu J, Wang J, Liu S, Yang J, Zhang G, Xiong Y, Li Z, Mao L, Zhou C, Zhu Z, Chen R, Hao B, Zheng W, Chen S, Guo W, Li G, Liu S, Tao M, Wang J, Zhu L, Yuan L, Yang H (2002) A draft sequence of the rice genome (*Oryza sativa* L. ssp. indica). **Science** 296: 79–92

Zee SY (1972) Vascular tissue and transfer cell distribution in the rice spikelet. **Aust J Biol Sci** 25: 411–414

Zhang WH, Zhou Y, Dibley KE, Tyerman SD, Furbank RT, Patrick JW (2007) Nutrient loading of developing seeds. **Funct Plant Biol** 34: 314–331